Light deflection in gadolinium molybdate ferroelastic crystals

2000 J. Phys.: Condens. Matter 12 669

(http://iopscience.iop.org/0953-8984/12/5/314)

J. Phys.: Condens. Matter **12** (2000) 669–676. Printed in the UK PII: S0953-8984(00)08245-X

Light deflection in gadolinium molybdate ferroelastic crystals

Piotr Staniorowski† and Jean Bornarel‡

† Institute of Experimental Physics, University of Wroclaw, PI. M. Borna 9 PL 50-204 Wroclaw, Poland

‡ Université Joseph Fourier - Laboratoire de Spectrométrie Physique, (UMR 5588) BP 87 - 38402 Saint-Martin-d'Hères Cedex, France

Received 29 September 1999

Abstract. The deflection of a He–Ne light beam by polydomain gadolinium molybdate (GMO) crystals has been studied with respect to incidence angle α_i on the sample at room temperature. The A and B deflected beams do not cross each other during the α_i variation, in contrast to results and calculations previously published. The model using the Fresnel equation confirms this result. The model presented is more accurate for numerical calculation than that using the Huygens construction.

1. Introduction

Light deflection occurs when a laser beam crosses a polydomain ferroelastic crystal due to the orientation difference of the optical indicatrices in adjacent domains. In the simplest case, only a permissible wall orientation (Fousek and Janovec 1969, Sapriel 1975) appears in the crystal and the largest face of the plate-shaped sample is perpendicular to the domain walls. If a non-polarized laser beam hits the plane perpendicular to the domain walls and to the largest sample face, six transmitted beams can be observed for incidence angle α_i: the direct beam D and the reflected beam R (on the domain walls) are non-polarized. The other beams are linearly polarized with the same polarizing plane of A and A′ perpendicular to the polarizing plane of B and B′. If the incidence angle α_i is smaller than the α_{cri} value only the D, R, A and A′ beams are observed. When α_i equals zero, D and R merge and only three transmitted beams are observed. This phenomenon has been described and explained in the previous paper (Bornarel *et al* 2000), where results in $(NH_4)_2SbF_5$ crystals (APFA) are studied. A review on previous works has also been published in 1993 (Tsukamoto and Futama 1993). Bornarel *et al* (2000) give a model using the Fresnel equation. This model allows one to simply demonstrate the linear dependence between the birefringence and $\sin\alpha^2$ (α is the A deflected angle) when the birefringence is equal to 10^{-2} or less. It is also shown that simultaneous measurements of the deflected angles and of the polarization of the light beams are necessary for a good knowledge of the crystal optical properties. The purpose of this paper is to clarify the discrepancies which exist in previous papers in gadolinium molybdate $Gd_2(Mo_4)_3$ crystals (GMO). The following section describes the experimental procedure. In section three, all of the information necessary to obtain accurate results on deflection angles versus α_i are given: the correlation between the deflection, the diffraction and the domain texture. The analytical model published in Bornarel *et al* (2000) allows us to explain the results here expressed. The A and B light beams do not cross each other in GMO, contrary to results previously published (Tsukamoto *et al* 1984). The numerical calculations performed using the Fresnel equation are

0953-8984/00/050669+08$30.00

more accurate than those using the Huygens construction, as explained in the last section of this paper.

2. Experimental procedure

GMO is ferroelectric and ferroelastic at room temperature and belongs to the orthorhombic point group *mm2* (Aizu *et al* 1969). GMO crystals exhibit an improper transition at 432 K between the orthorhombic phase and a tetragonal high-temperature phase, which is paraelectric. The permissible walls are in the (100) and (010) planes. The crystallographic a and b axes in the polydomain orthorhombic phase interchange with each other in the adjacent domains. The mutual inclination angle of the indicatrices in the adjacent domains is $2\phi = 90^\circ$ in section (001) (ϕ is the angle between the slow neutral line and the domain wall in the (001) section, as shown in figure 2 of Bornarel *et al* (2000)).

Good quality crystals of GMO with poled boule-shape are obtained by the Czochralski process. Samples were cut in the form of thin plates perpendicular to the c ferroelectric axis. The orientation of sample faces were verified with x-ray Bragg diffraction (accuracy of 1 arc min) and each face was polished with 0.1 μm diamond paste on a silk cloth. The thickness of studied samples varies between 1 mm and 10 mm, but for the sake of clarity all of the results presented here correspond to a sample of a 2 mm thickness. The domain texture of the sample is accurately studied with the help of an Orthoplan–Leitz microscope ($\times$320 magnification). Then the deflection experiments are performed at room temperature with the help of a goniometer, which was built in the laboratory. It is possible, using a He–Ne, 632 nm laser as a light source, to rotate the sample with regard to the incident laser beam, step-by-step, with an accuracy of 0.05°. This is the best possible accuracy on the α_i angle. The deflected angle is determined with the aid of an automatically-rotated photodiode with the same theoretical accuracy: but as explained in the following section, the intensity distribution of the transmitted beams allows, in the best cases, to obtain an accuracy on the deflected angles α (A beam) and β (B beam) equal to 0.2°. Due to the width of the light beam and the sample thickness, the typical uncertainty on the α value, for α_i equal 40°, is equal to 0.4°. Finally the polarization of the light beams is also measured, with an accuracy of 0.3°.

3. Results

The intensity distributions of the transmitted beams are given in figures 1 and 2. These explain how to obtain the best measurements of the α and β angles in the GMO crystals. These distributions are drawn against the angle θ' between a transmitted beam and the D beam position at an incidence angle $\alpha_i = 0$. In figure 1 the sample is translated so that the region crossed by the laser beam corresponds to different domain textures: in figure 1(a) the laser beam meets a dense and regular domain texture; in figure 1(b) the number of domain walls met by the laser beam is still large, but the domain widths are irregular; and in figure 3(a) the laser beam meets only a few non-equidistant domain walls. In the case shown in figure 1(a) the transmitted light distribution is similar to the Frauenhofer diffraction pattern obtained with a grating. The mean angle difference between the two adjacent maxima $\Delta\theta'$ corresponds to a mean domain width equal to 45 μm (Hill and Ichiki 1964, Ha and Kim 1985). This domain width value is well verified by microscopic observations. It is also possible in figures 1(a)–1(b) to observe the diffraction effect due to the elementary domain shape itself. The diffraction phenomena becomes quasi-negligibly related to the deflection

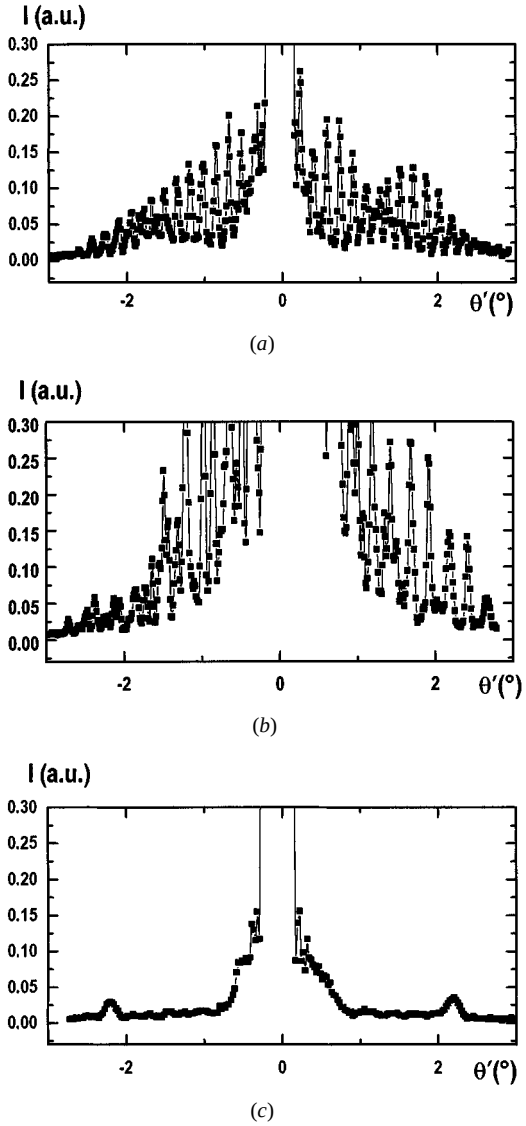

Figure 1. The transmitted light pattern with incidence angle α_i equal to zero in three situations of the GMO domain texture: (*a*) dense and regular domain texture; (*b*) a great number of domain walls with poor periodicity; and (*c*) a few non-equidistant domain walls.

phenomena in the case of a few domain walls at different distances between themselves, as illustrated in figure 1(*c*). Then, it is this case which is chosen to measure the deflexion phenomena in GMO and corresponds to the other results reported here. For example, figure 2 shows the deflected beam intensities for different values of the α_i angle. In figure 2(*a*), $\alpha_i = 0$ and the A and A′ beam intensities appear with a few hundredth of the value of the directly transmitted beam's D('s) intensity. When α_i increases and remains smaller than the critical value α_{cri} (see figure 2(*b*)), the R beam appears and the A and A′ beam intensities change. These modifications of beam intensities is an interesting research subject (Meeks and Auld 1988), but not the aim of the present paper. If α_i becomes greater than α_{cri} as in

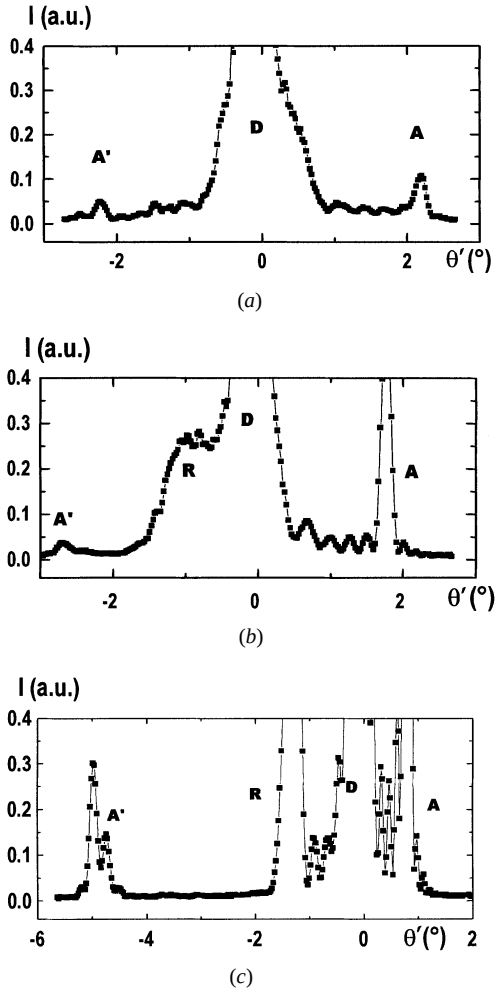

Figure 2. The transmitted light pattern with a few domain walls (*a*) $\alpha_i = 0^\circ$; (*b*) $\alpha_i < \alpha_{cri}$; and (*c*) $\alpha_i > \alpha_{cri}$.

figure 2(*c*), the B and B′ beams appear. It is possible to note that in GMO their appearance induces a strong decrease of the R and A′ beam intensities, almost unobservable in figure 2(*c*). Figure 2 illustrates the distribution of light when α_i is smaller than 50°. For greater values the intensities of the deflected beams decrease and the accuracy on their angles (α and β) becomes worse.

The variation at room temperature of the α and β angles against the α_i angle is plotted in figure 3. An enlargement is given around the value $\alpha_i = 9.6^\circ$ where it has been previously predicted that the A and B beams interchange (Tsukamoto *et al* 1984). Also, the modification of the A and B beams' polarization is drawn in figure 4. The polarization orientations of the A and B beams change strongly when α_i varies between 0° and 20° with an inflexion point near 9–10°. A and B beam polarizations remain perpendicular to each other for all α_i values.

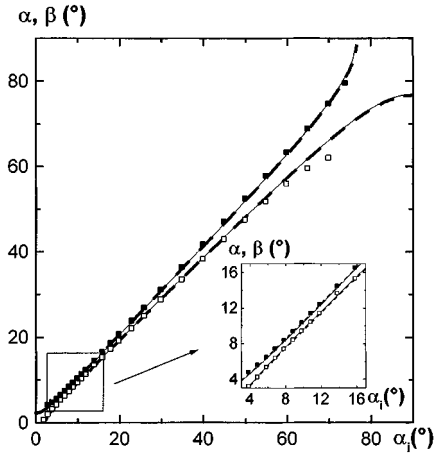

Figure 3. Variation of the α (■) and β (□) deflected angles against α_i, calculated values by the general model (full curve) and by the approximated model (broken curve). The insert gives the detailed data in the enlargement region.

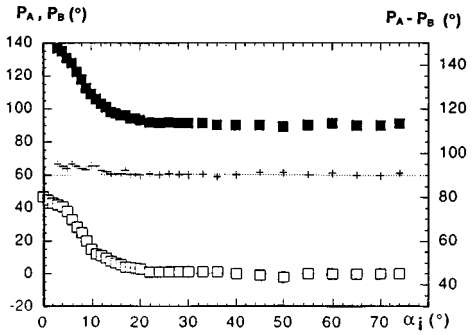

Figure 4. Variation of the deflected beam polarization (■ and □ correspond to the results of figure 3, respectively).

4. Discussion

The variation of the deflected angles α and β on the incidence angle α_i can be calculated in the same way as in Bornarel *et al* (2000). The principal axes for the susceptibility are the orthorhombic axes with the optical indices $n_x = 1.8500$, $n_y = 1.8504$, $n_z = 1.900$ (Aizu *et al* 1969). The domain wall is in the $(y'z')$ planes, which is a tetragonal plane, and the incident plane is perpendicular to the domain wall direction as illustrated in figure 5(*a*) ($\phi = 45^\circ$). The index surfaces are shown in figure 5(*b*). Figures 6–8 and relation (3) of Bornarel *et al* (2000) must be changed by the permutation $x \to y$, $y \to z$, $z \to x$. As in APFA case, it is possible to calculate $\alpha(\alpha_i)$ and $\beta(\alpha_i)$ and these numerical results are plotted in figure 3 (full curve). It is also possible to consider the intersections between the index surfaces and the incident plane as ellipses in a primary approximation. By the same way as in Bornarel *et al* (2000), the $\alpha(\alpha_i)$

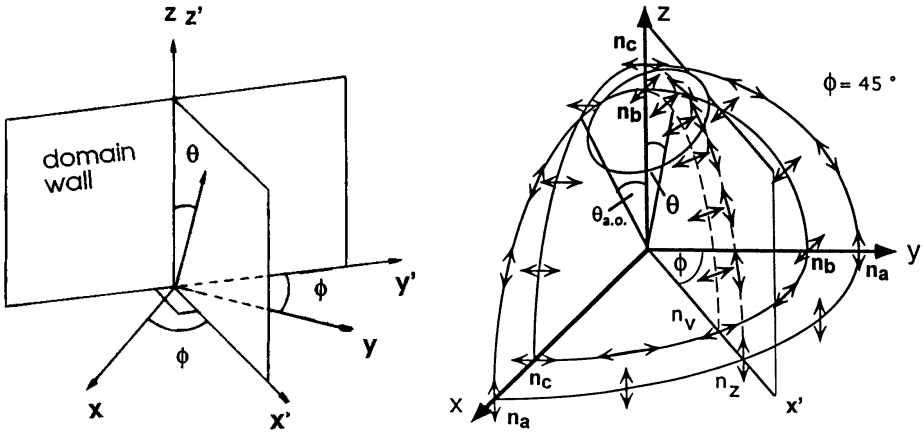

(*a*) (*b*)

Figure 5. (*a*) The principal axes for the susceptibility χ: x, y and z; the domain wall $(y'z)$ and the incident plane $(x'z)$ are shown. (*b*) The index surfaces in GMO with the incident plane $(x'z)$ (the situation is the same for both permissible walls).

and $\beta(\alpha_i)$ relations can be obtained in this approximated model:

$$\alpha = \pm \arcsin \frac{n_z}{n_y}\left(\frac{(n_x^2/n_y^2)\mathrm{tg}^2\phi + 1}{\mathrm{tg}^2\phi + 1}\sin^2\alpha_i + n_y^2 - n_x^2\right)^{1/2} \tag{1}$$

$$\beta = \pm \arcsin\left[\frac{\mathrm{tg}^2\phi + 1}{(n_x^2/n_y^2)\mathrm{tg}^2\phi + 1}\left(n_x^2 - n_y^2 + \frac{n_y^2}{n_z^2}\sin^2\alpha_i\right)\right]^{1/2} \tag{2}$$

giving $\alpha(0^\circ) = \alpha_{cri} = 2.2^\circ$, in good agreement with the experimental measurements.

The curves $\alpha(\alpha_i)$ and $\beta(\alpha_i)$ corresponding to the relations (1) and (2) are drawn (broken curves) in figure 3. Figure 6 give the difference between the experimental data and the theoretical data for $\alpha(\alpha_i)$ and $\beta(\alpha_i)$, as well as the difference between the simplified model data and the general model data. The simplified model is a good approximation in all of the α_i range for the $\beta(\alpha_i)$ variation, and is also good for $\alpha(\alpha_i)$, except in the vertical tangent region (α_i greater than 70°). The accuracy of the experimental data equals a few tenths of a degree of arc for the α_i angle between 3° and 40°. For smaller α_i values the deflected beams are close to the undeflected beam D and, without deconvolution, the uncertainty can be 0.5° or more. For α_i values greater than 40°, the light intensity of the A and B beams decreases. Furthermore, the thickness of the sample plays an important role, on the one hand, because of the usual lateral displacement of the laser beam and, on the other hand, due to the greater number of crossed domain walls, which complicate the transmitted light pattern. To obtain more accurate measurements it would be necessary to use a thinner sample, a more powerful collimated laser and to study the intensity light distribution against the crossed domain wall number. However, the purpose of this work was to study, especially, the region around 9–10°, as this is the α_i region where the measurement accuracy is the best. Then the experimental measurements, as the calculated data, demonstrate that the $\alpha(\alpha_i)$ and $\beta(\alpha_i)$ curves do not cross each other. The modification of the light beam polarization (shown in figure 4) is clearly understandable with the help of figure 5(*b*): the incident plane (zx') (or (zv)) forms a large angle (45°) with the principal optical plane (zx) which contains the optical axis. However, when the α_i value is between 5° and 15°, the region of the index surfaces crossed by the $\vec{k}$ vectors is in fact near the optical axis. It explains why the A and B beam polarizations exhibit such strong

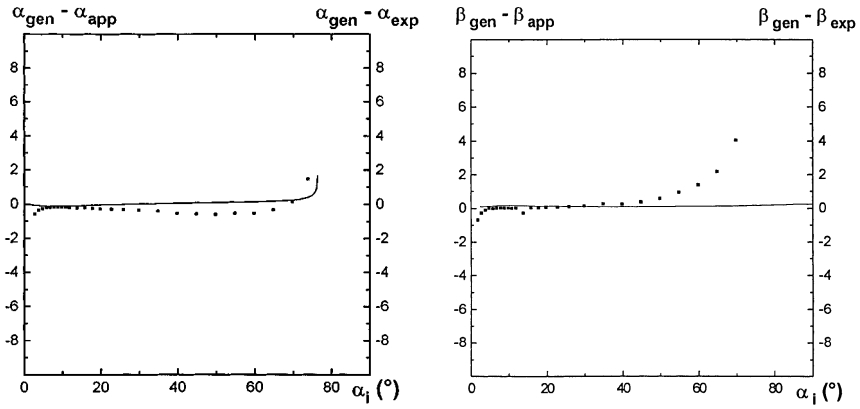

(*a*) (*b*)

Figure 6. The difference between the deflection angle values calculated by the general model and the experimental data (■), and the approximated model (full curves). (*a*) $\Delta\alpha(\alpha_i)$ and (*b*) $\Delta\beta(\alpha_i)$.

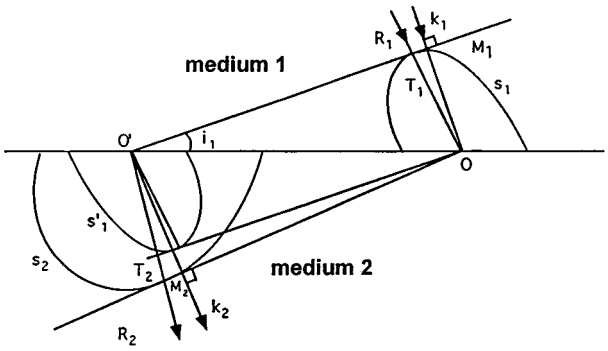

Figure 7. The principle of the Huygens construction.

variations. More precisely the curves exhibit inflexion points when $\alpha_i = 9.6°$, which allows one to know the angle between the optical axis and the z-axis in the principal optical plane (zx). This is a good illustration of the deflection measurement: it is possible, with preliminary measurement of the ϕ angle and with $\alpha(\alpha_i)$ and $\beta(\alpha_i)$ curves, to determine optical properties of crystals. Why does the calculation process described here give better results than that using the Huygens construction (Tsukamoto *et al* 1984)? In both cases, the same values for n_x, n_y, n_z and ϕ were used. The Huygens construction process predicts a crossing of the A and B beams and the process presented allows the calculation, with good accuracy, of the $\alpha(\alpha_i)$ and $\beta(\alpha_i)$ variations. This process clearly shows, even with the ellipsoid approximation, that A and B beams do not cross each other. It is easy to illustrate the different accuracies with the help of figures 7 and 8 of Bornarel *et al* (2000) and figure 7. The knowledge of the n_x, n_y and n_z values is not perfect and so, as a consequence, the calculated index surfaces, wave surfaces and slowness curves. In the case of the Huygens construction (see figure 7), a plane parallel to the incident wave (T_1O') and tangent to the wave surface S'_1 is built. Then the point O is determined. After that another plane which contains O and tangent to the wave surface S_2 is built. The point T_2 and the $\vec{k}_2$ vector are determined. Any error in the n_x, n_y and n_z values is then, on the wave surface shapes, amplified by the drawing of the tangent planes. This is

not the case in the model presented in paper I where the $\vec{k}$ vector is obtained with the help of projections on the index surfaces as illustrated in figures 7 and 8 of paper I. Simulations performed with small variations in the n_i values confirm this analysis.

5. Conclusion

The deflection angles α and β, which correspond to the A and B beams, respectively, were measured against the incidence angle α_i at room temperature in GMO crystals. The A and B beams do not cross each other as previous papers predicted. A model explains these results, even using a simplified manner. This process is better for numerical calculations than that using the Huygens construction.

The deflection phenomena in GMO crystals is often mingled with the diffraction by the domain walls, due especially to the value of the tilt angle ϕ (equal to 45°). Further works in GMO crystals on the transmitted light pattern would be interesting, but they need very accurate measurements because of the small intensities of the deflected beams in this crystal.

References

Aizu K, Kumada A, Ashida S and Yumoto H 1969 *J. Phys. Soc. Japan* **27** 511
Bornarel J, Staniorowski P and Czapla Z 2000 *J. Phys.: Condens. Matter* **12** 653
Fousek J and Janovec V 1969 *J. Appl. Phys.* **40** 1 135
Ha D H and Kim J J 1985 *Japan. J. Appl. Phys.* **24** 556
Hill R M and Ichiki S K 1964 *Phys. Rev.* A **135** A1640
Meeks S W and Auld B A 1988 *Adv. Electron. Electron. Phys.* **71** 251
Sapriel J 1975 *Phys. Rev.* B **12** 5128
Tsukamoto T and Futama H 1993 *Phase Trans.* **45** 59
Tsukamoto T, Hatano J and Futama H 1984 *J. Phys. Soc. Japan* **53** 838